FLUID FLOW IN MANIFOLD GEOMETRIES - AN EXPERIMENTAL AND THEORETICAL STUDY

by

M Langsholt and D Thomassen
Institute for Energy Technology

Paper 4.2

NORTH SEA FLOW METERING WORKSHOP 1988
18-20 October 1988

National Engineering Laboratory
East Kilbride, Glasgow

FLUID FLOW IN MANIFOLD GEOMETRIES - AN EXPERIMENTAL AND THEORETICAL STUDY.

Morten Langsholt and Dag Thomassen

Institute for Energy Technology, Box 40, 2007 Kjeller, Norway

S U M M A R Y

A gas metering station based on orifice meters normally consists of a number of parallel meter-runs between headers. Some disturbances, e.g. swirl, decay slowly and since such disturbances may significantly change the orifice discharge coefficient, accurate measurements rely on properly designed upstream headers.

This paper presents results from measurements of mean velocities and turbulence intensities in a plexiglass model of a gas metering station. The flowing fluid was atmospheric air. Various pipe-configurations upstream of the inlet header have been examined and differences are highlighted. The results illustrate clearly the strong connection between metering station design and the flow conditions (swirl, skewness etc.) at the inlet of the meter-runs.

In addition to the measurements the paper also presents some results from numerical simulation of fluid flow in 3-D manifold geometries. These simulations have been performed using the program Phoenics.

NOTATION

D - header diameter
k - directional sensitivity coefficients in response equation
k - turbulent kinetic energy (defined by eq. 3)
Tu - turbulence intensity (eq.4)
U - velocity in x-direction in fixed coordinate system
u - fluctuating component of velocity in x-direction
$\overline{U}$ - average velocity in x-direction in fixed coordinate system
V - velocity in y-direction in fixed coordinate system
v - fluctuating component of velocity in y-direction
$\overline{V}$ - average velocity in y-direction in fixed coordinate system
W - velocity in w-direction in fixed coordinate system
w - fluctuating component of velocity in w-direction
$\overline{W}$ - average velocity in w-direction in fixed coordinate system
U_{eff} - effective cooling velocity
U_{ax} - typical axial velocity, see eq.4
V_N - velocity components in wire-oriented coordinate system
V_T - velocity components in wire-oriented coordinate system
V_B - velocity components in wire-oriented coordinate system

Subscripts:

B - axis normal to wire and normal to probe axis
N - axis normal to wire and normal to axis 'B'
T - axis parallel to wire

1. INTRODUCTION

A gas metering station will normally consist of at least two parallel meter tubes connected to a header. Accurate flow measurement depends on the meter being properly designed, manufactured, installed and operated. The geometry and its tolerances are regulated through the standard ISO-5167.

The standard requires fully developed turbulent profiles to exist at the inlet of the meter. The means to fulfill this requirement is to introduce a long straight pipe upstream of the meter. The required minimum straight lengths vary according to the nature of the nearest upstream fitting and with the diameter ratio of the orifice meter. The minimum straight lengths are given in the standard. However, questions have been raised to the validity and consistency of the given tables. There are also problems in interpreting the standard when components not included in the standard (e.g. headers) are used.

It might well be that the header design creates a flow disturbance which persist much longer than the disturbance traceable to a valve closer to the meter. This illustrates one important problem faced when designing a metering station, and it explains our interest in manifold flow.

Over the last few years we have at IFE been interested in the potential role of Computational Fluid Dynamics as a research and/or design tool for gas metering stations. So far promising results have been achieved for a numerical model for flow through an orifice plate. This model proved to be sensitive, and accurate, to even small alterations in inlet profile, plate geometry etc.

A long term goal is to be able to simulate numerically the flow field that will appear in the meter-runs for a given metering station design. In this way various alternative configurations can be compared and inappropriate ones avoided. A prerequisite is of course to be able to simulate the flow through a header.

The background for the experimental work presented in this paper was to establish experimental evidence so that proper evaluation of a numerical model for simulation of flow in a header geometry could be performed.We decided to limit the verification to a header design with two parallel meter runs, as illustrated in Figure 1.

A plexiglass model of a gas metering station with upstream header of this design was built and interfaced with an air flow rig. Detailed measurements of velocity and turbulence profiles at the inlet of the header and in the entrance section of the meter tubes have been performed by use of hot-wire techniques. Measurements were conducted for various pipe configurations upstream of the header inlet plane.

Subsequent to the experimental work identical cases were modelled in the numerical model and the results compared with the experimental data.

2. THE EXPERIMENTAL WORK

2.1 The flow rig

The IFE air flow rig is an atmospheric rig where a positive displacement pump sucks air through the test section. The static pressure in the loop is therefore slightly below the atmospheric pressure. The capacity of the pump is approximately 0.45 m^3/s.

In the experiments described here the test section was made up by the "metering station", including the immediate upstream geometry, connected to the pump as shown in Figure 2.

The test section

The fixed part of the test section consisted of the gas metering station with its two parallel meter runs. The inlet and outlet headers had an internal diameter of 190 mm (D), while the two meter runs had an internal diameter of 96 mm, see Fig.1. The pipes were made of transparent plexiglass with hydraulically smooth walls. No flow metering device was mounted in the meter runs. The Reynolds number in the meter-runs was $1.5*10^5$.

The exchangeable part of the test section, denoted the inlet geometry, was the piping immediately upstream of the inlet header. Three different inlet geometries were examined :

Designation:	Description of inlet geometry:
Inlet no. 1	straight pipe (20 D)
Inlet no. 2	single 90^0 bend + straight pipe (10 D)
Inlet no. 3	2 x 90^0 offset bend + straight pipe (10 D)

The sections of straight pipe of the inlet geometries were plexiglass pipes with 190 mm internal diameter. The bends had an internal diameter of 182 mm and a wall roughness exceeding that of the plexiglass pipes. The radius of curvature for the bends was 1.5 D.

2.2 Instrumentation

Hot-wire anemometry

The main instrument for measuring the mean flow velocity components and the turbulent kinetic energy was a tsi manufactured Constant Temperature Hot-wire Anemometer. The probe used was a single slanted (45^0) wire. The anemometer signal was digitized and reduced in an IBM PC AT compatible computer using a software package also delivered by tsi.

From the hot-wire instrument one obtains an effective cooling velocity, U_{eff}, which is a measure of the heat transport off the wire. By statistical analysis on a sample of readings of U_{eff}'s one find an average term and a fluctuating term. Through the sensor response equation, which defines the relation between the actual velocity and the effective cooling velocity, one can invert the problem to determine the mean velocities and the velocity fluctuations.

We did use the response equation :

$$U_{eff}^2 = k_N^2 V_N^2 + k_T^2 V_T^2 + k_B^2 V_B^2 \qquad \text{(eq.1)}$$

The instantaneous velocity components in the fixed XYZ-coordinate system can be written as the sum of a mean and a fluctuating part:

$$U = \overline{U} + u \; ; \; V = \overline{V} + v \; ; \; W = \overline{W} + w \qquad \text{(eq.2)}$$

The turbulent kinetic energy, k, is defined as :

$$k = \frac{1}{2} (u^2 + v^2 + w^2) \qquad \text{(eq.3)}$$

The response equation (eq.1) combined with the data reduction method of Acrivlellis (Ref./2,3/) gave us the mean velocity components and the turbulent kinetic energy in each point of measurement.

Pitot-static tube

As a reference velocity measurement for the calibration of the hot-wire anemometer we used a pitot static tube. The differential pressure was measured with a Type 5, Airflow testing set. For inlet geometry no.1 and no.2 the pitot static tube was also used to measure the axial velocity component along all 4 traverses.

2.3 Measurement procedure

The aim of the experiments was to measure the velocity field and the turbulent kinetic energy in a number of points in the inlet plane and in the two outlet planes of the header shown in Figure 1.

In the inlet plane the points of measurement were located along both the vertical and the horizontal diameter. Along each traverse measurements were performed in 8 positions. In the outlet planes measurements were made in 4 positions along the vertical diameter only.

As is also indicated in Figure 1, the vertical traverse in the inlet plane is denoted traverse "A", the horizontal one "B". The traverse in the outlet plane nearest to the inlet is called "C", and the remaining one "D". We also frequently refer to the outlets as outlet "C" and outlet "D", respectively.

At each of the four wall entry points a ruler was fixed against which the axial probe position was read. In addition an angular ruler was fixed to the probe support for angular positioning of the probe. This experimental set-up is shown in Figure 3. In each point of measurement along each traverse we operated the probe at typically 9 different rotational angles. This was done partly to close the set of equations

(independent information), but also to reduce the effect of measurement uncertainty. The method of multipositioning the wire(s) to procure the required amount of information is based on the assumption of a "stationary" turbulent flow-field.

2.4 Results from the measurements

General

When we analyzed the measurement results it proved obvious that the measurements for inlet geometry no.3 was imperfect and had to be encumbered with additional measurement uncertainty. This inlet geometry typically generates strong swirl and high turbulence intensities, a situation which represent a challenge for the measurement system. Numerical experiments performed indicated that for variations in the inlet profile, within the limits of measurement uncertainty, the outlet flow regime could change significantly for example from twin vortices to a single vortex. The results for inlet geometry no.3 will therefore neither be the presented nor discussed.

The mean velocity vectors found have been decomposed into an axial component and a lateral one. The lateral component is represented by the vector-arrows in Figures 4 and 5. The point of attack for the vector is located on the mid-point of the arrow, and the vector-scale is given individually for each cross-section. The point of observation is on the downstream side. (For orientation of the fixed coordinate axes, see Fig. 1.) The axial velocity components are represented on the figures simply by their numerical values.

The turbulent kinetic energy will not be treated in detail for reasons that will become clear later in the paper.

The axial velocity profiles have been found both from the hot-wire measurements and from the pitot static tube measurements (i.e. two independt measurement techniques). The two sets of axial profiles compare well both in the inlet plane and in the two outlet planes.

Inlet plane

For inlet no.1 in Figure 4, the lateral velocities measured were in general smaller than the measurement uncertainty and are not included in the presentation. The axial velocities exhibit a typical parabolic profile. The skewness observed along traverse "B" are probably an effect of outlet "C" which is only 1 D downstream of the measurement section.

For inlet no.2 we clearly see in Figure 5 two secondary vortices superposed on a fairly skew axial profile.

The turbulence intensities, Tu, were relatively moderate, spanning from typically 6% for the straight pipe inlet geometry to values up to 20% for the inlet consisting of a single bend. The following definition of the turbulence intensity has been used :

$$Tu = \sqrt{2k} / U_{ax} \qquad \text{(eq.4)}$$

Outlet planes

In outlet "D" of Figure 4 there seems to exist two vortices symmetrically located about the horizontal mid-plane and for the same outlet in Figure 5 we can definitely identify a relatively strong single vortex. This vortex was also detected by a two-bladed turbine of zero pitch installed 1.5 D downstream of the metering plane. The turbine was never installed when hot-wire measurements were performed.

In outlet "C", for both inlets, the lateral velocity vector showed more or less identical behaviour. The vertical component was directed downwards (positive x-direction) and the horizontal component was directed to the right (the negative z-direction).

The measured axial velocity profiles in the outlet planes showed a parabolic shape with minimum velocity near the pipe centre-line.

The turbulence intensities found were for outlet "C" in the range 15-30% with the highest values near the centre-line. For outlet "D" the values were in the range 15-20 %. There was no significant difference between the intensities found for the various inlet geometries.

3. THE NUMERICAL SIMULATIONS

3.1 The Phoenics code

This is a general purpose fluid dynamic computer program based on a numerical solution algorithm developed at the Imperial College in London. The code is made commercially available through the company CHAM, ltd. For description of the program see refs./6,7/

3.2 Description of the numerical model

The grid

The manifold geometry is modeled in a cartesian coordinate system by "blocking" out cells from an initially rectangular bar. This leads to a manifold consisting of rectangular ducts. These rectangular ducts are approximated to circular pipes by the use of so-called porosity functions. These functions enable fractions of cell-volumes and cell-surfaces to be made unavailable for the fluid.

Polar coordinates, which appear to be a more natural choice when describing circular pipes, could not be used due to the coupling of pipes perpendicular to each other.

The computation domain was divided into a 12x20x27 grid (NXxNYxNZ) as illustrated in Figure 6. Of all these cells, approximately one half have been completely blocked out using the porosity functions.

The dependent variables

The equations were solved with respect to the following 5 dependent variables :

- 3 velocity components,
- the pressure and
- the density.

Boundary conditions

At the inlet plane profiles for all solved for variables, except for the pressure, were prescribed. Three different sets of profiles were established on the basis of the hot-wire measurements, one for each of the inlet geometries.

The outlet boundary was a fixed pressure boundary.

Due to the smoothing process of the rectangular ducts described above, wall-functions could not be activated for any of the dependent variables. One consequence of this is that the no-slip condition for velocities at the pipe-wall is neglected.

No turbulence model

In the present version of the numerical model we have no turbulence model and all viscous forces with origin in the turbulent velocity fluctuations are therefore neglected.

3.3 Results of the simulations

In this presentation we will focus on the solution found in the two outlet planes. The situation in the inlet plane does anyway only reflect the inlet conditions prescribed.

In Figure 7 and 8 we present the converged solution found in the two outlet planes for inlet geometries no.1 and 2. Also included in these figures are the measured velocity components.

There are two "windows" drawn for each outlet plane, one presenting the lateral velocities and the other one iso-lines for the axial velocities. The vector-plot (to the left), shows the velocity vectors projected into the outlet plane (lateral velocities). The vectors drawn in bold-face types represent the measured velocity vectors, while the remaining represent the simulations. The point of attack for the vectors is their mid-point and the vector scale is indicated below the figure.

The right hand "window" shows iso-lines for the axial velocities simulated, the numbers indicate the velocities for the iso-curves. The filled circles indicate the point of measurement with the hot-wire and the corresponding velocities found are given to the right at the same level as the circles.

The square shape of the drawn cross-sections, instead of a circle, is a result of the geometry modelling using blockages on square ducts.

4. Discussion

Effect of no turbulence model

We decided not to use a turbulence model since the use of standard turbulence model gave unrealistic outlet flow fields. This may be ascribed to the lack of proper boundary conditions the turbulence model variables.

No turbulence model in the computations means that the inertia forces dominates the flow. In our case this seems to be a realistic assumption due to our high Reynold numbers and since the fluid experiences large accelerations from inlet to outlet.

We also did numerical tests to examine the effect on the velocity field in the header when assuming no turbulence model. Only minor changes were observed and the assumption was accepted as valid.

The outlet planes for inlet geometry no.1 (Figure 7)

For outlet "C" we could, in the numerical solution, see the existence of a recirculation zone with point of reattachment close to the position of the defined outlet plane. Therefore we regard this case to be a difficult task for the hot-wire anemometer. As can be seen from Figure 7 a) the measured lateral velocities does not fit very well to the simulations. Concerning the axial profile, we can see that the simulations predict minimum velocities near the pipe-axis, although not as pronounced as for the measurements.

In outlet "D" the lateral velocities compare as well as could be expected. The axial velocities are too high, but show the desired typicality of minimum velocity near the center-line.

The outlet planes for inlet geometry no.2 (Figure 8)

The lateral velocities compare very well for outlet "D" and acceptable for outlet "C". One must keep in mind the measurement uncertainty, estimated to 1.0-1.5 m/s, for the lateral velocities.

For the axial profiles we can not explain the observed differences by measurement uncertainty. The numerical model, therefore, fails to predict the axial profiles in this case. Examination of the numerical solution 2D downstream of the point of measurement showed, however, much better agreement with the measurements. It appears as if typical features of the flow need longer distances to develop in the numerical model than what is found in the measurements. The absence of the effective viscosity of the turbulence in the numerical model may explain this effect.

5. CONCLUSIONS

1. It is possible to simulate numerically the flow in headers, however, to a considerable computer time cost.

2. The available calculational tool did not enable proper no-slip wall boundary conditions and turbulence treatment.

3. Tests did show that these simplifications to the numerical model were not critical to the results.

4. The best agreement is reached when the inlet profile is generated by a simple geometry generating the smallest turbulence level. This, of course, gives the best precision of the inlet profile measurement and consequently also for the inlet boundary condition for the numerical model.

5. We are convinced that the computational tool can be further developed and verified to become a valuable tool in design work.

Future work

This work is continued. The measurement system is improved and more traverses will be taken. The inlet boundary conditions to the header model will be generated by a separate straight pipe or bend simulation.

ACKNOWLEDGEMENTS

The work has been financially supported by Statoil a.s.We wish to thank Dr. Karl Sjøen at Statoil for his help and advice throughout the work.

6. REFERENCES

/1/ Jørgensen,F.E.: "Directional sensitivity of wire and Fiber-film probes." DISA Information No.11, 1971.

/2/ Acrivlellis,M.: "Hot-wire measurements in flows of low and high turbulence intensity." DISA Information no.22, 1977.

/3/ Acrivlellis,M.: "Finding the spatial flow field by means of hot-wire anemometry." DISA Information no.22, 1977.

/4/ Langsholt,M.:"3-D numerical simulation of fluid flow in manifold geometries using the Phoenics computer code", IFE/KR/F-87/069.

/5/ Langsholt,M. and Thomassen,D. :"Computer modelling of fluid flow through orifices", Flow Measurements in the Mid 80's, Conference held at NEL, 9-12 june 1986.

/6/ Spalding,D.B. et al. PHOENICS instruction manual. CHAM TR/100,1986.

/7/ Spalding D.B.:"A general purpose computer program for multi-dimensional one and two-phase flow." Mathematics and Computers in Simulation North Holland Press, vol XXlll, pp 267-276, (1981)

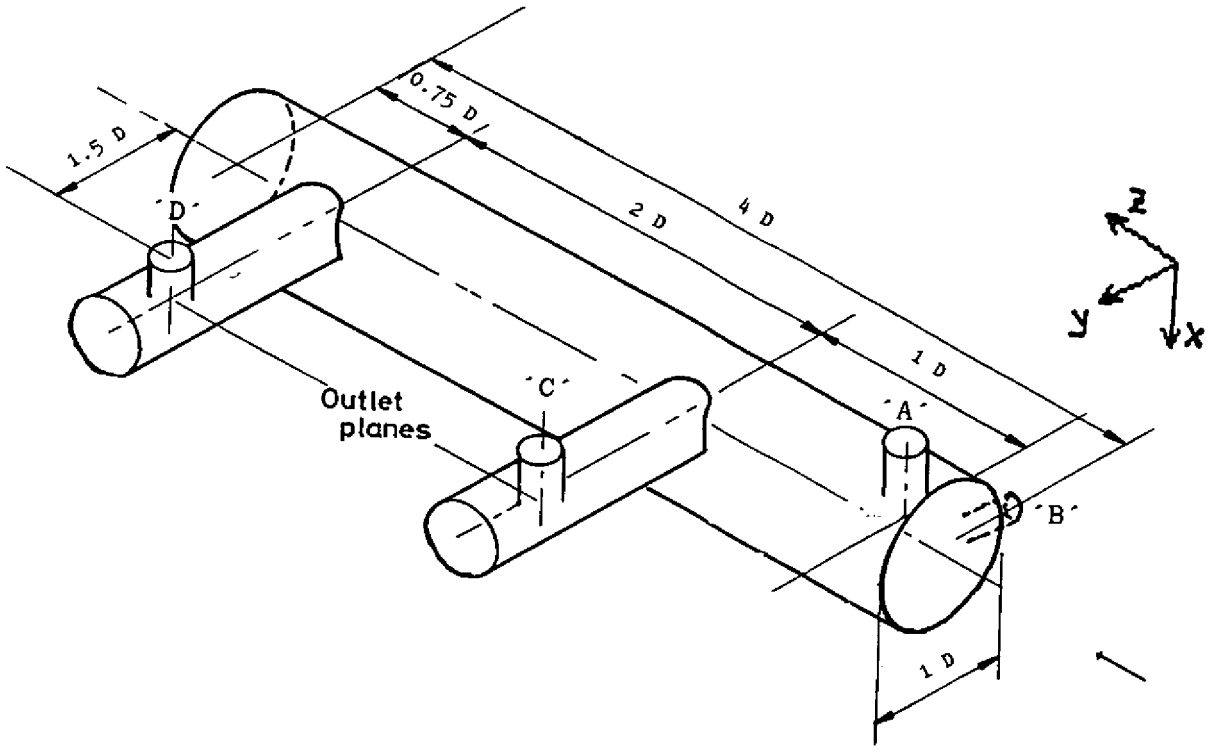

Figure 1. The header geometry.

Figure 2. The experimental set up with inlet geometry no.3 mounted.

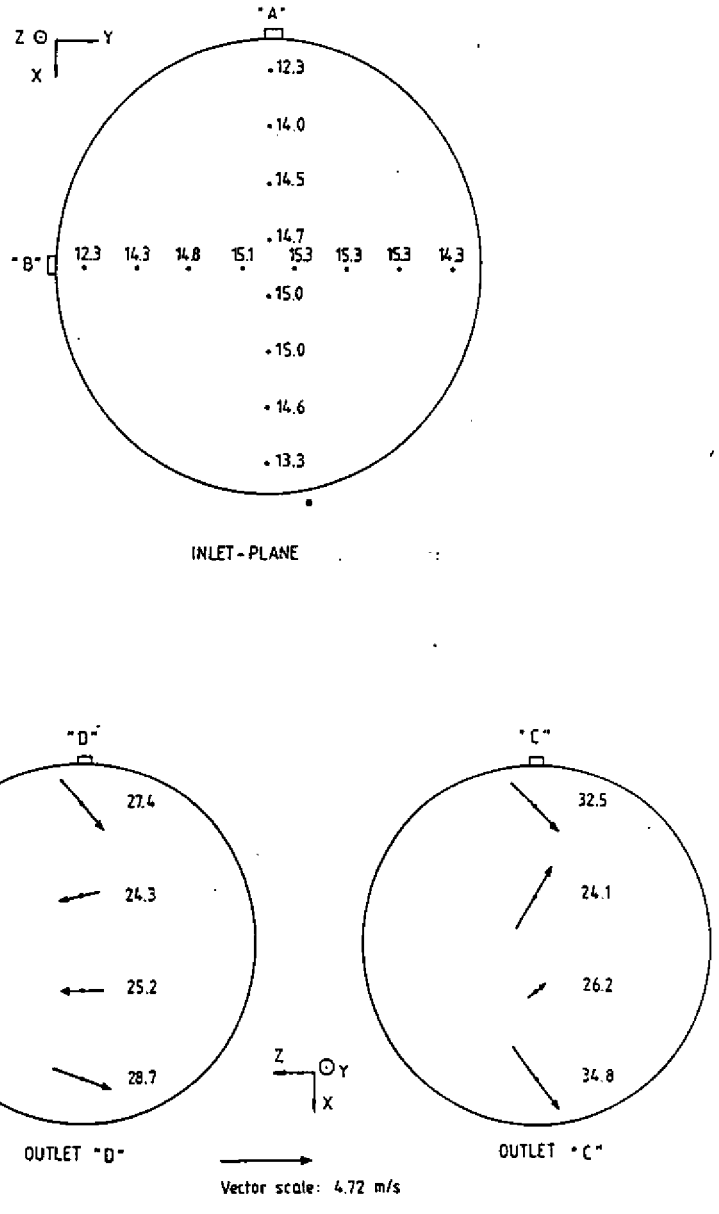

Figure 4. Vector plot presenting the lateral velocity vector measured in the inlet and outlet planes for inlet geometry no.1. The numerical values relate to the axial velocity component.

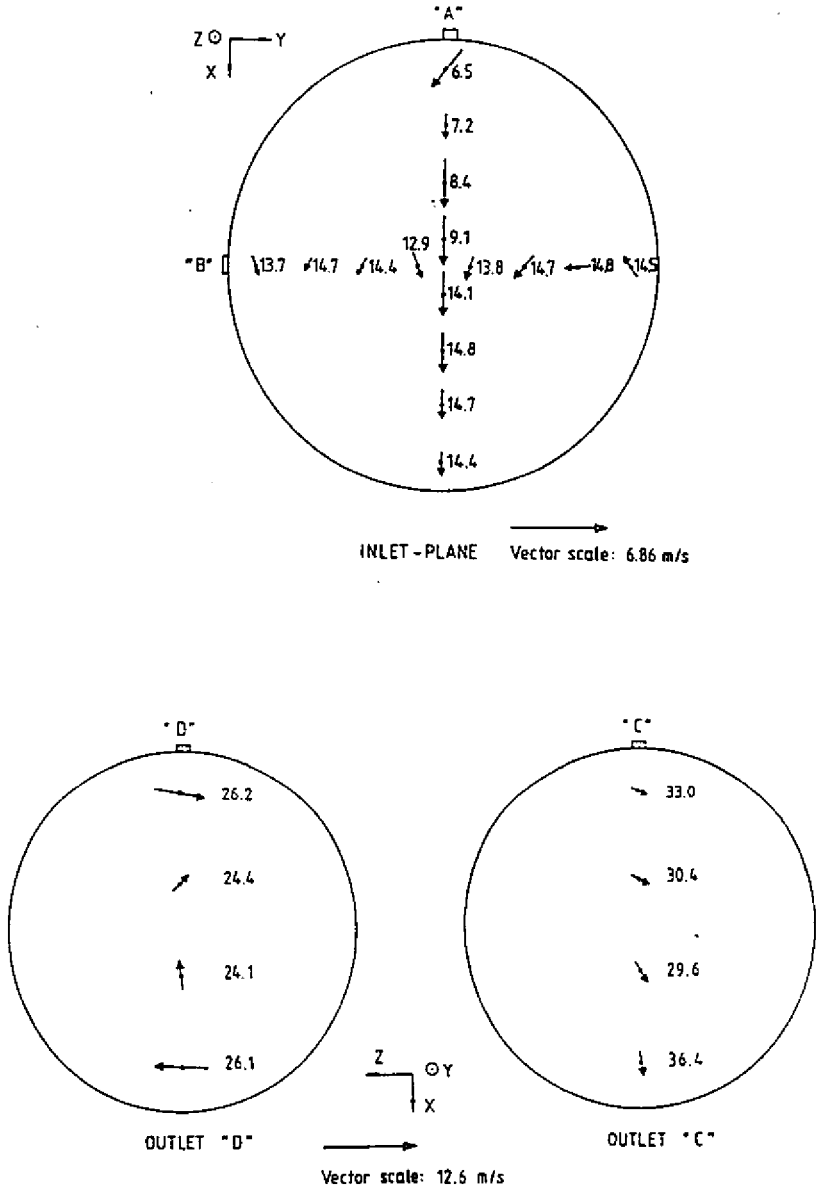

Figure 5. Vector plot presenting the lateral velocity vector measured in the inlet and outlet planes for inlet geometry no.2. The numerical values relate to the axial velocity component.

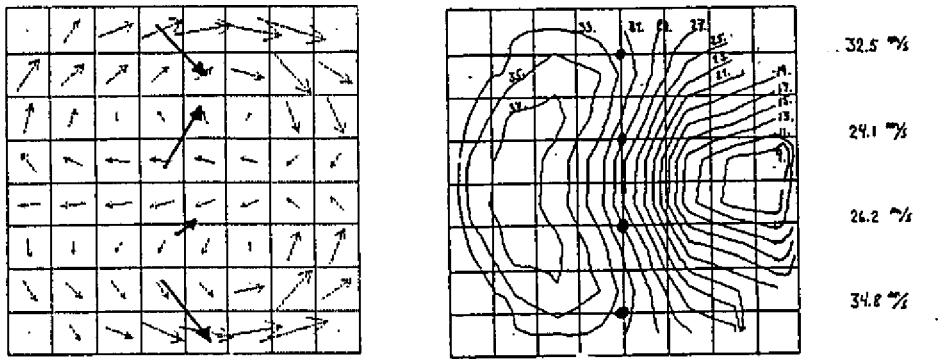

a) outlet "C"

Vector scale: 4.72 m/s

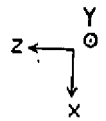

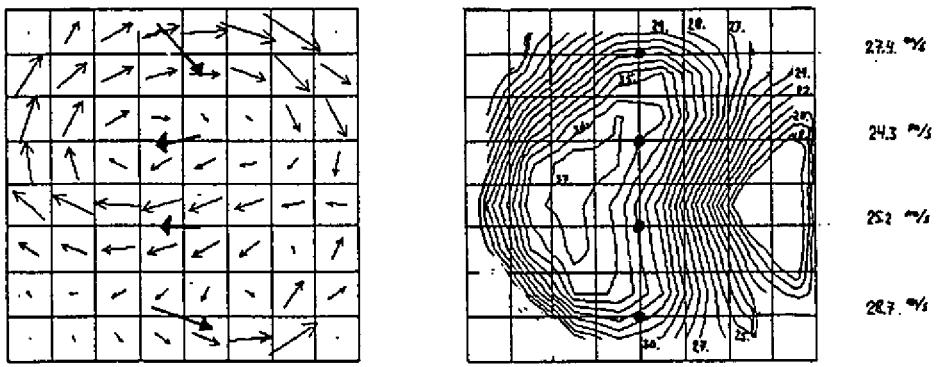

b) outlet "D"

Figure 7. Velocity fields in the two outlet planes for inlet geometry no.1. Both measurements and simulations.

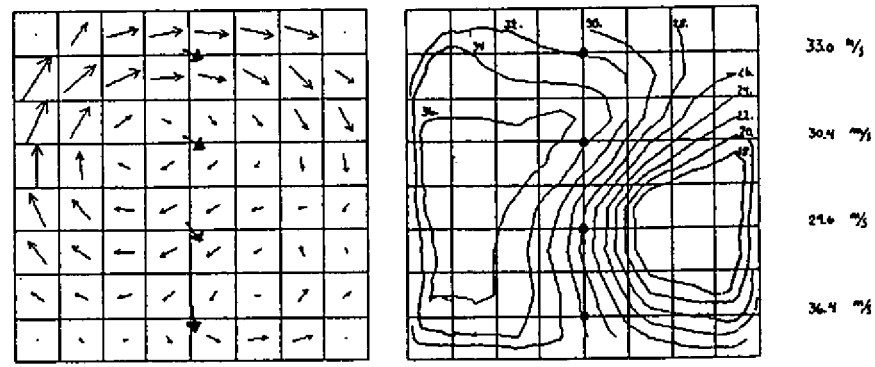

a) outlet "C"

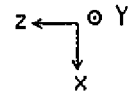

Vector scale: 12.6 m/s

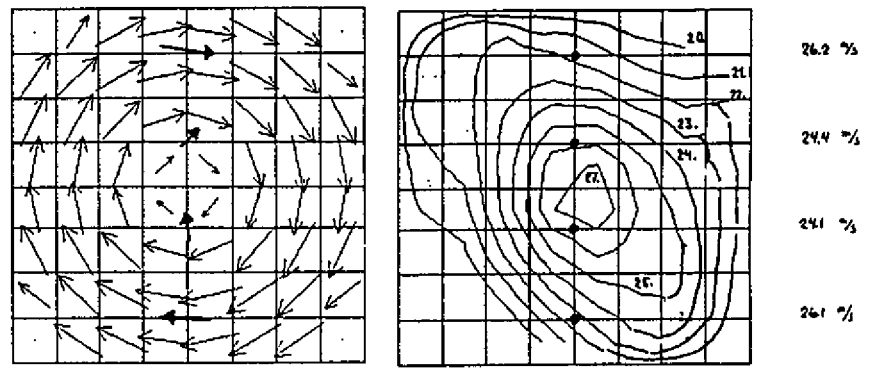

b) outlet "D"

Figure 8. Velocity fields in the two outlet planes for inlet geometry no.2. Both measurements and simulations.